Neurotoxicity Research (2019) 36:175–192
https://doi.org/10.1007/s12640-019-00042-w

ORIGINAL ARTICLE

Caffeic Acid Phenethyl Ester (CAPE) Protects PC12 Cells Against Cisplatin-Induced Neurotoxicity by Activating the AMPK/SIRT1, MAPK/Erk, and PI3k/Akt Signaling Pathways

Rafaela Scalco Ferreira[1] · Neife Aparecida Guinaim dos Santos[1] · Carolina P. Bernardes[1] · Flávia Malvestio Sisti[1] · Lilian Amaral[1] · Andreia C.K. Fontana[2] · Antonio Cardozo dos Santos[1]

Received: 2 October 2018 / Revised: 26 March 2019 / Accepted: 4 April 2019 / Published online: 23 April 2019

Abstract

Peripheral sensory neuropathy (PSN) is a well-known side effect of cisplatin characterized by axonal damage. In the early stage of neurotoxicity, cisplatin affects proteins that modulate neurite outgrowth and neuroplasticity, without inducing mitochondrial damage or apoptosis. There are no preventive therapies for cisplatin-induced peripheral neuropathy; therefore, measures to improve axonal growth and connectivity would be beneficial. Caffeic acid phenethyl ester (CAPE) is a bioactive component of propolis with neurotrophic and neuroprotective activities. We have recently showed that CAPE protects against cisplatin-induced neurotoxicity by activating NGF high-affinity receptors (trkA) and inducing neuroplasticity. We have now assessed other potential early targets of cisplatin and additional mechanisms involved in the neuroprotection of CAPE. Cisplatin reduced axonal cytoskeletal proteins (F-actin and β-III-tubulin) without inducing oxidative damage in PC12 cells. It also reduced energy-related proteins (AMPK α, p-AMPK α, and SIRT1) and glucose uptake. At this stage of neurotoxicity, glutamate excitotoxicity is not involved in the toxicity of cisplatin. CAPE attenuated the downregulation of the cytoskeleton and energy-related markers as well as SIRT1 and phosphorylated AMPK α. Moreover, the neuroprotective mechanism of CAPE also involves the activation of the neurotrophic signaling pathways MAPK/Erk and PI3k/Akt. The PI3K/Akt pathway is involved in the upregulation of SIRT1 induced by CAPE, but not in the upregulation of cytoskeletal proteins. Altogether, these findings suggest that the neuroprotective effect of CAPE against cisplatin-induced neurotoxicity involves both (a) a neurotrophic mechanism that mimics the mechanism triggered by the NGF itself and (b) a non-neurotrophic mechanism that upregulates the cytoskeletal proteins.

Keywords Cisplatin · Neurotoxicity · Axonal regeneration · CAPE · Neuroprotection · Neurotrophic signaling · Peripheral neuropathy

Introduction

Cisplatin is an effective chemotherapeutic drug used for the treatment of several types of cancer; however, it induces several toxicities, with neurotoxicity being the major dose-limiting side effect. Cisplatin induces a distal dose-dependent symmetrical sensory neuropathy that affects 30–40% of patients who complete a full course of chemotherapy and is associated with cumulative doses of 350 mg/m^2 (Johnson et al. 2015; Shirmanova et al. 2017; Kanat et al. 2003). The sensory symptoms have a "stocking and glove" distribution characterized by sensory loss, numbness, tingling, or paresthesia in fingers and/or toes and decreased distal vibratory sensitivity (Argyriou et al. 2012; Park et al. 2008). These symptoms may persist for several months and can progressively worsen over time, even after the treatment has ended, a phenomenon called "coasting" (Siegal and Haim 1990). Long-term neuropathy lowers the quality of life of many cancer patients and leads to discontinuation of treatment resulting in suboptimal cancer treatment (Areti et al. 2014).

✉ Antonio Cardozo dos Santos
acsantos@fcfrp.usp.br

[1] Department of Clinical Analyses, Toxicology and Food Sciences, School of Pharmaceutical Sciences of Ribeirão Preto, University of São Paulo, Ribeirão Preto, SP, Brazil

[2] Department of Pharmacology and Physiology, Drexel University College of Medicine, Philadelphia, PA, USA

Post-mortem analyses of the neural tissue of chemotherapy patients have revealed the accumulation of cisplatin in the sensory neurons of the dorsal root ganglion and in the peripheral sensory nerves. Such accumulation seems to remain indefinitely as actively toxic, which is consistent with the coasting phenomenon. The brain and the spinal cord are protected from the accumulation of cisplatin by the presence of the blood–brain barrier (Gregg et al. 1992); however, there is growing evidence that CNS metastases cause BBB disruption favoring the passage of drugs into the CNS (Inno et al. 2016). The main mechanism associated with cisplatin-induced neurotoxicity is the formation of platinum adducts in the nuclear and mitochondrial DNA of primary sensory neurons, causing their death by apoptosis (McDonald et al. 2005; Podratz et al. 2011). However, it might also be associated with mechanisms not directly related to DNA damage. The pathogenesis of peripheral neuropathy is related to a retrograde axonal degeneration that might progress to neuronal apoptosis (Asbury 1987; Krarup-Hansen et al. 2007). In fact, one of the most important signs in the early stages of neuronal apoptosis is neurite retraction (Sadri et al. 2010). Nevertheless, the precise mechanism underlying cisplatin-induced neurotoxicity is not known (Starobova and Vetter 2017). At the later stages, the cell body and axons might be irreversibly lost; however, at the earlier stages, the cell body has not been damaged yet, and the axonal degeneration could be reversible by discontinuation of treatment or even regenerated (Asbury 1987). Studies have proposed the exogenous administration of neurotrophic factors as a strategy to protect injured neurons and stimulate axonal regeneration in both the central and peripheral nervous systems (Lykissas et al. 2007). Based on this premise, we have previously demonstrated the neurotrophic and neuroprotective activities of caffeic acid phenethyl ester (CAPE) against the axonal damage induced by cisplatin in PC12 cells, a model of sympathetic neurons responsive to NGF. The study showed that CAPE induces neuroplasticity through activation of NGF high-affinity receptors (trkA) and upregulation of axonal proteins related to neurite outgrowth and synaptic communication (Ferreira et al. 2017). Therefore, we have now assessed the involvement of the two main cascades activated by trkA receptors (MAPK/Erk and PI3k/Akt pathways) in the mechanism of neuroprotection of CAPE. Besides that, we evaluated the effects of CAPE and/or cisplatin on other targets that have been associated with the pathology of the peripheral nervous system, such as cytoskeleton, bioenergetics, oxidative status, and glutamate uptake (Carozzi and Ceresa 2012; Stevens et al. 2000; Prior et al. 2017).

Materials and Methods

Chemicals

High-purity reagents (analytical-grade minimum) were obtained from Sigma-Aldrich® (St. Louis, MO, USA), unless differently stated. Cell culture media were purchased from Invitrogen (Carlsbad, CA). Reagents for Western blot analyses were obtained from Bio-Rad Laboratories, Inc. (Hercules, CA, USA). Radiolabeled substrates, deoxy-D-glucose 2-[1,2-^{3}H(N)] (1.0 μCi), L-[^{3}H]-glutamate (51.1 Ci/mmol), liquid scintillation cocktail (Ultima Gold™), and aqueous-based solubilizer (SOLVABLE™) were purchased from PerkinElmer (Boston, MA, USA). DL-TBOA (DL-threo-beta-benzyloxyaspartate) was purchased from Tocris (Bristol, UK). Transfection reagent TransIT-LT1 was from Mirus Bio LCC (Madison, WI). The solutions were prepared with ultrapure water (type I) purified in a Milli-Q gradient system (Millipore, Bedford, USA). The stock solution of cisplatin (3.3 mM) was prepared in 0.9% saline solution, and the stock solution of CAPE (100 mM) was prepared in DMSO and stored in a freezer (− 20 °C).

Cell Cultures

All the assays, except for the glutamate uptake assays, were performed in PC12 cells. The glutamate assays were performed in transfected COS-7 cells, transfected HEK cells, and glial cells, which naturally express the glutamate transporters EAATs.

PC12 Cells

PC12 cells were obtained from the American Type Culture Collection (ATCC, Rockville, MD) and were cultured in 75 cm^2 culture flasks at 37 °C under a humidified atmosphere containing 5% CO_2 and 95% air. The growth medium was Dulbecco's Modified Eagle's Medium (DMEM; GIBCO®) supplemented with 10% heat-inactivated horse serum (GIBCO®), 5% heat-inactivated fetal bovine serum (FBS; GIBCO®), and 1% antibiotic mixture (5 mg/mL penicillin, 5 mg/mL streptomycin, and 10 mg/mL neomycin, PNS GIBCO®). Medium was renewed every 3 days. For cell harvesting, the medium was removed and the cells were detached with trypsin/EDTA solution (GIBCO®). Trypsin was inactivated by the addition of supplemented medium; after centrifugation (1000 rpm, 5 min), the cells were suspended in the growth medium and plated at the appropriate density of each assay.

For differentiation assays, the growth medium was replaced by the differentiation medium composed of F-12K Nutrient Mixture Kaighn's Modification (GIBCO®) supplemented with 1% horse serum and 1% antibiotic mixture (penicillin/neomycin/streptomycin, PNS, GIBCO®).

COS-7 Cells

COS-7 cells (American Type Culture Collection (ATCC), Manassas, VA 20110, USA) were cultured in 150 cm^2 flasks

in Dulbecco's Modified Eagle's Medium (Invitrogen Life Technologies, Carlsbad, CA, USA) containing 10% fetal bovine serum, 100 units/mL of penicillin, and 100 μg/mL of streptomycin in a humidified incubator with 5% CO_2 at 37 °C. Upon reaching confluence, the media was aspirated and the cells were rinsed with PBS prior to the incubation with trypsin (for 15 min at 37 °C). Fresh DMEM was added to inactivate the trypsin, and, then, the cell suspension was split 1:2 in 150 cm^2 flasks and incubated (37 °C, 5% CO_2) until the assays.

HEK Cells

HEK cells stably transfected with EAAT2 (kindly provided for Susan G. Amara, Pittsburgh) were cultured at 37 °C in 150 cm^2 flasks in Dulbecco's Modified Eagle's Medium (Invitrogen Life Technologies, Carlsbad, CA, USA) supplemented with 10% fetal bovine serum, penicillin (100 units/mL), streptomycin (100 μg/mL), and hygromycin (100 μg/mL) in a humidified atmosphere with 5% CO_2. Upon reaching confluence, the media was aspirated and the cells were washed with PBS and trypsinized for 15 min at 37 °C. Fresh DMEM was added to the flasks to inactivate the trypsin, and, then, the cell suspension was split (1:2) and incubated until the assays.

Glial Cells

All animal experiments were treated according to the guidelines for the use of animals in research approved by the Drexel University Institutional Animal Care and Use Committee (IAUCUC) and are in agreement with the US Public Health Service Policy on Humana Care and Use of Laboratory Animals. Glia was prepared and cultured according to a previous study (Shimizu et al. 2011), with modifications. Briefly, cerebral cortices from 2- to 4-day-old Holtzman rat pups were dissected under sterile conditions and placed in 60 mm dishes containing dissection medium (in mM: 16 glucose, 22 sucrose, 135 NaCl, 5 KCl, 1 Na_2HPO_4, 0.22 KH_2PO_4, 10 HEPES, pH 7.4, osmolarity 310 + 10 mOsm). Tissue was minced with curved scissors and digested in 0.25% trypsin for 15 min. Trypsin activity was ended by transferring tissue pieces to another vial with dissection medium. Tissue was then repeatedly aspirated/dispensed with a serological pipette until dissociation, centrifuged for 15 min at 280 g, resuspended in glia plating medium (90% DMEM, 10% FBS, and 50 μg/mL gentamicin), transferred to culture 150 cm^2 flasks, and incubated at 37 °C (5–10% CO_2) for 10 days before plating in 96-well plates.

Working Concentrations of Cisplatin and CAPE

The working solution of cisplatin (5 μM) was prepared in saline solution, and the working solution of CAPE (10 μM) was prepared in the differentiation medium (F-12K Nutrient Mixture Kaighn's Modification supplemented with 1% horse serum) immediately before the assays. The concentrations were determined in our previous studies (Ferreira et al. 2016; Ferreira et al. 2017).

Inhibition of NGF Signaling Pathways (PI3k/Akt and MAPK/Erk)

PC12 cells (2.0×10^5 cells/well) were seeded in 24-well plates coated with poly-L-lysine (Sigma-Aldrich®, St. Louis, MO, USA) and incubated for 24 h at 37 °C for adhesion. Then, the medium was replaced by the differentiation medium. The cells were pretreated for 1 h with one of the following inhibitors: 30 μM LY294002 (blocks PI3k/Akt pathway) or 10 μM U0126 (blocks MAPK/Erk pathway). Then, the cells were incubated (37 °C, 72 h), with one of the following additions: NGF 100 ng/mL or CAPE 10 μM. Untreated cells were used as controls. The neurite outgrowth was assessed by inverted-phase contrast microscopy (Carl Zeiss Axio Observer A1 inverted microscope, 400× magnification). Phase-contrast photomicrographs of four fields per well were taken after incubation for 72 h. The percentage of cells with neurites was determined in the digitalized images by using the ImageJ open-source software (Rasband 1997–2018). Only those cells with at least one neurite with a length equal to or greater than the diameter of the cell body were considered differentiated (Das et al. 2004).

Western Blot Analysis (F-Actin, β-III-Tubulin, SIRT 1, AMPK α, and p-AMPK α)

Preparation of Cell Lysate

For determination of F-actin and β-III-tubulin, PC12 cells (2×10^5 cells/well) were seeded in 24-well, poly-L-lysine-coated microplates, whereas for determination of SIRT 1, AMPK α, and p-AMPK α, PC12 cells (5×10^5 cells/well) were seeded in 12-well, poly-L-lysine-coated microplates. In both cases, the cells were incubated for 24 h at 37 °C for adhesion. Then, the growth medium was replaced by the differentiation medium. The cells were incubated (37 °C, 72 h) with one of the following additions: NGF 100 ng/mL, CIS 5 μM + NGF 100 ng/mL, CAPE 10 μM, or CAPE 10 μM + CIS 5 μM + NGF 100 ng/mL. Untreated cells were used as controls. After the treatment, the cells were detached with trypsin, transferred to centrifuge microtubes, and centrifuged (1000 rpm, 5 min, 4 °C). The supernatant was discarded, and the cell pellet was suspended in 40 μL CelLytic lysis buffer (Sigma-Aldrich®, St. Louis, MO, USA) containing 1:200 Protease Inhibitor Cocktail and 1% Phosphatase Inhibitor Cocktail. The lysis procedure was performed with tubes placed on ice to reduce the activity of proteases. After

10 min, the cell lysate was centrifuged at 12,000 rpm for 10 min at 4 °C and the supernatant was stored in freezer (− 80 °C) until the assays. Cell lysate (10 μL) was assayed for t protein content by the Bradford's method.

Determination of Protein in Cell Lysate (Bradford)

The Protein Assay Dye Reagent (Bio-Rad) was used according to the manufacturer's instructions. Lysates and color reagent were diluted with water (1:5), and a calibration curve of BSA (40, 100, 200, and 400 μg/mL) was assayed. The absorbance (595 nm) was determined in a microplate reader (Multiskan FC, Thermo Scientific). The concentration of protein was calculated based on the calibration curve and multiplied by the dilution factor (5).

SDS-Polyacrylamide Gel Electrophoresis and Transfer

Samples were added to an equal volume of Laemmli sample buffer (65.8 mM Tris, pH 6.8, 26.3% glycerol, 2.1% SDS, 0.01% bromophenol blue, 5% β-mercaptoethanol) and heated to 98 °C for 5 min. Aliquots of 25 μL containing 10 μg total protein were applied to 10% polyacrylamide gel (10 wells) and separated by SDS-polyacrylamide gel electrophoresis (SDS-PAGE) (1 h, 160 V, Tris/glycine/SDS buffer).

Proteins were transferred to nitrocellulose membranes (1 h, 0.37 A, Tris/glycine buffer).

Blocking and Incubation with Antibodies

Membranes were blocked (30 min, room temperature, 300 rpm) with 5% non-fat milk or 5% BSA in Tween 20/TBS buffer (TTBS). Membranes were incubated with the following primary antibodies: mouse anti-F-actin (1:100) or rabbit anti-β-III-tubulin (1:1000), both obtained from Abcam (Cambridge, MA, USA), or rabbit anti-SIRT 1 (1:1000), rabbit anti-AMPK α (1:500), or rabbit anti-FOSFO-AMPK α (1:500), obtained from Sigma-Aldrich® (St. Louis, MO, USA), overnight, at 4 °C, 300 rpm. Then, the membranes were washed with TTBS and incubated (1 h, room temperature, 300 rpm) with the secondary antibody conjugated with horseradish peroxidase (anti-mouse IgM or anti-rabbit IgG; HRP 1:20,000). The membranes were washed with TTBS and TBS and treated with 3 mL of chemiluminescence enhancer detection reagent (1:1). Images were captured by using ChemiDoc system (Bio-Rad Laboratories, Inc., Hercules, CA, USA). Quantitation was performed on the images based on the optical densitometry (OD) of the bands by using the ImageJ open-source software (Rasband 1997–2018). Finally, the membranes were stripped (2% SDS, 62.5 mM Tris pH 6.8 and 100 mM mercaptoethanol) and reprobed for loading control (anti-β-actin 1:3000). OD values of the test protein bands were divided by the OD values of the loading control for result normalization (L'Episcopo et al. 2011).

Glucose Uptake

PC12 cells were seeded in 12-well plates coated with poly-L-lysine (Sigma-Aldrich®, St. Louis, MO, USA) at a density of 1.0×10^6 cells/well and incubated for 24 h, at 37 °C for adhesion. Cells were treated with one of the following additions: CIS 5 μM, CAPE 10 μM, or CIS 5 μM + CAPE 10 μM and incubated for 72 h (37 °C 5% CO_2). Untreated cells were used as controls. Then, the medium was removed, the wells were washed twice with PBS (phosphate-buffered saline), followed by the addition of 1 mL of glucose-free DMEM (GIBCO®). For positive controls, the cells were incubated (1 h/37 °C) with cytochalasin B (10 μM; Sigma-Aldrich®, St. Louis, MO, USA), a potent inhibitor of glucose transport (Ebstensen and Plagemann 1972). Then, all the groups were incubated with a solution containing 1.0 μCi 2-[1,2-^{3}H(N)] deoxy-D-glucose and unlabeled glucose (50 μM), for 30 min at 37 °C. The solution was removed, the cells were washed with PBS (3×), lysed with 200 μL of SOLVABLE™ (PerkinElmer; Boston, MA, USA) for 10 min, followed by the addition of 1 mL scintillation cocktail Ultima Gold™ (PerkinElmer; Boston, MA, USA). The homogenized cell suspension of each well was transferred to microtubes. The scintillation was determined in a Microbeta 1450 LSC Luminescence Counter (PerkinElmer, Waltham, MA), and the results were expressed as counts per minute (CPM) (Abdul Muneer et al. 2011).

Measurement of Intracellular ROS Generation

The levels of intracellular reactive oxygen species (ROS) were determined by using the dichloro-dihydro-fluorescein diacetate (DCFH-DA) assay, modified from a previous study (Liu et al. 2013). Briefly, PC12 cells were seeded into 96-well plates (1.0×10^5 cells/well) coated with poly-L-lysine (Sigma-Aldrich®, St. Louis, MO, USA) and incubated for 24 h for adhesion. Then, the medium was replaced by serum-free F-12K Nutrient Mixture Kaighn's Modification (GIBCO®) and the cells were incubated with 100 μM DFCH-DA (30 min/37 °C). After the incubation, the medium was removed, the cells were washed twice with PBS, following addition of 300 μM H_2O_2, 5 μM CIS, 10 μM CAPE, or 5 μM CIS + 10 μM CAPE (72 h, 37 °C). The medium was removed again, and the cells were washed twice with PBS and lysed with 50 μL SOLVABLE™ (PerkinElmer; Boston, MA, USA). The homogenized cell suspension was transferred to black 96-well plates, and the fluorescence intensity was determined at 485 nm (excitation)/520 nm (emission).

Transient Transfection and Glutamate Uptake in COS-7 Cells

COS-7 cells were maintained in DMEM containing 10% fetal bovine serum, penicillin (100 units/mL) and streptomycin (100 μg/mL) in a humidified atmosphere with 5% CO_2 at 37 °C. Cells were transfected transiently with cDNAs of excitatory amino acid transporter (EAAT2) or with empty vector pCMV-5 (to obtain the background). For glutamate uptake assays, subconfluent COS-7 cells were seeded (5.0×10^4 cells/well) in 24-well tissue culture plates and transfected with 0.5 μg of plasmid DNA per well using TransIT-|LT1 transfection reagent (Mirus Bio LLC). One day after transfection, the cells were incubated with different concentrations of cisplatin (0.48, 2.4, 12, 60, and 300 μM) for 30 min. Then, the media was removed and the cells were washed with 0.3 mL of PBS-CM (PBS plus 1 mM $CaCl_2$ and 0.1 mM $MgCl_2$). The uptake was initiated by the addition of 50 nM L-[^{3}H]-glutamate. Reactions were allowed to occur for 10 min, the cells were washed with PBS-CM twice, and, then, lysis buffer (1% SDS, 0.1 N NaOH) was added to the wells. Plates were placed on a plate rocker for 20 min, and cell homogenates were transferred to scintillation vials containing 3 mL of scintillation fluid. Radioactivity was quantified in a scintillation counter LS 6500 (Beckman Coulter, Brea, CA).

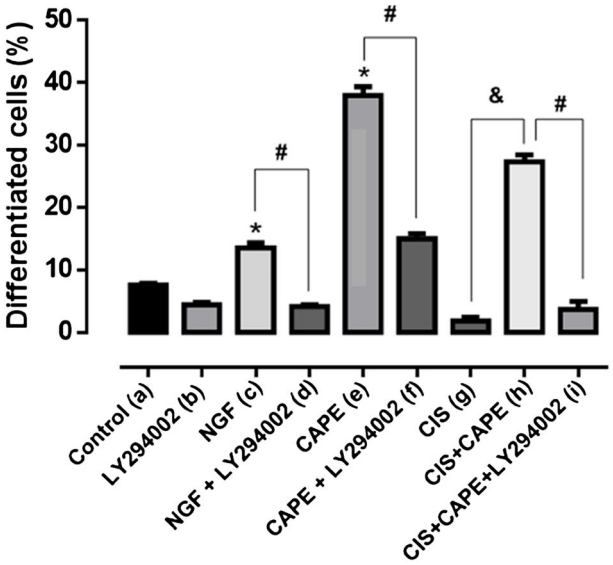

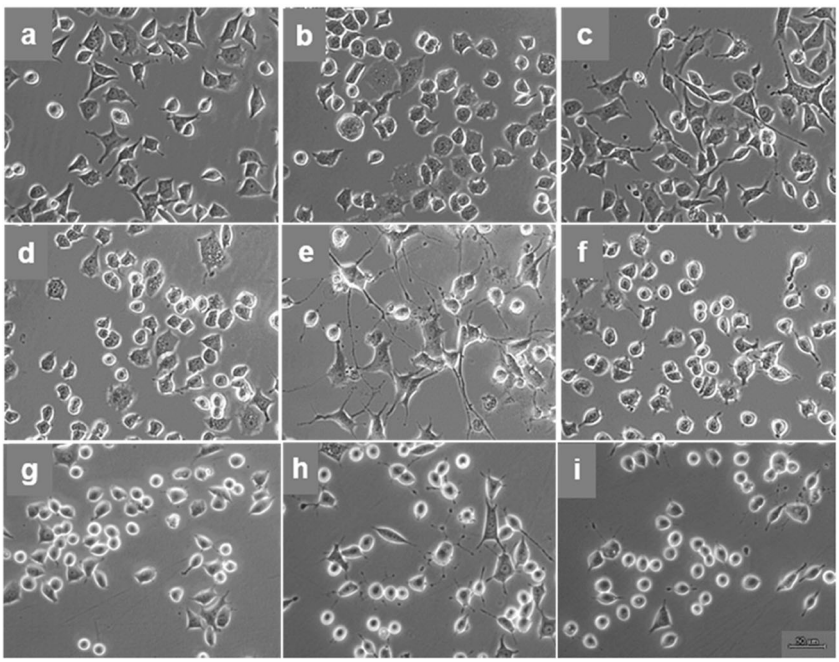

Fig. 1 Effects of the inhibitor of the PI3K/Akt pathway (LY294002) on the differentiation of PC12 cells exposed to cisplatin and/or CAPE. PC12 cells were pretreated with LY294002 (30 μM) for 1 h and then treated with 100 ng/mL NGF, 5 μM cisplatin, and/or 10 μM CAPE. Inverted phase-contrast photomicrographs of (**a**) controls (untreated cells); (**b**) inhibitor LY294002 30 μM; (**c**) NGF 100 ng/mL; (**d**) NGF + LY294002; (**e**) CAPE 10 μM; (**f**) CAPE + LY294002; (**g**) CIS; (**h**) CIS + CAPE; and (**i**) CIS + CAPE + LY294002 after incubation for 72 h. The number of cells with at least one neurite with the length equal to or higher than the cell body is expressed as percentage of the total cells in the field. Bars represent mean ± SEM of three different experiments performed in triplicates. *Significantly different from the untreated control group ($p < 0.05$); #significantly different from the respective control without inhibitor ($p < 0.05$); &significantly different from the cisplatin group ($p < 0.05$)

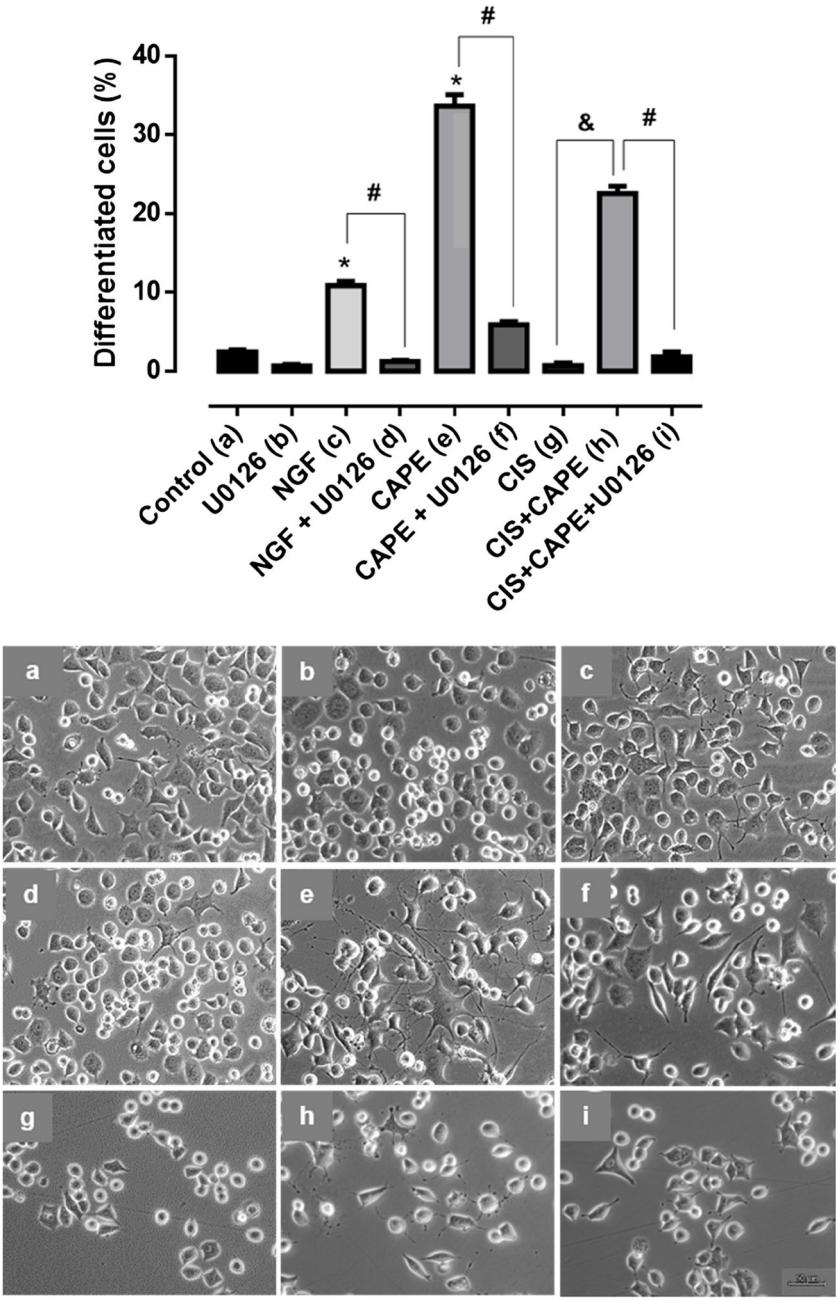

Fig. 2 Effects of the inhibitor of the MAPK/Erk pathway (U0126) on the differentiation of PC12 cells exposed to cisplatin and/or CAPE. PC12 cells were pretreated with U0126 (10 μM) for 1 h and then treated with 100 ng/mL NGF, 5 μM cisplatin, and/or 10 μM CAPE. Inverted phase-contrast photomicrographs of (**a**) controls (untreated cells); (**b**) U0126 10 μM; (**c**) NGF 100 ng/mL; (**d**) NGF + U0126; (**e**) CAPE 10 μM; (**f**) CAPE + U0126; (**g**) CIS; (**h**) CIS + CAPE; and (**i**) CIS + CAPE + U0126 after incubation for 72 h. The number of cells with at least one neurite with the length equal to or higher than the cell body is expressed as percentage of the total cells in the field. Bars represent mean ± SEM of three different experiments performed in triplicates. *Significantly different from the untreated control group ($p < 0.05$); #significantly different from the respective control without inhibitor ($p < 0.05$); &significantly different from the cisplatin group ($p < 0.05$)

Glutamate Uptake in Transfected HEK Cells—Stable Transfection

Subconfluent HEK cells were plated (5.0×10^4 cells/well) in 24-well tissue culture plates and incubated for 24 h at 37 °C for adhesion. MDCK-naïve cells were used as controls (non-transfected; do not express EAAT2). Cells were incubated with different concentrations of cisplatin (0.48, 2.4, 12, 60, and 300 μM) for 24, 48, and 72 h. After incubation, the medium was removed and the cells were washed with 0.3 mL of PBS-CM (PBS with the addition of 1 mM $CaCl_2$ + 0.1 mM $MgCl_2$). Uptake reactions were initiated by the addition of 50 nM L-[^{3}H]-glutamate. Reactions were allowed to occur for 10 min, and, then, the cells were washed with PBS-CM twice and lysed (1% SDS, 0.1 N NaOH). Plates were gently mixed on a plate rocker for 20 min, and, then, the cell homogenate was transferred to scintillation vials containing 3 mL of scintillation cocktail. The radioactivity was quantified in a scintillation counter MicroBeta Wallac 1450 (PerkinElmer).

Glutamate Uptake Assays in Glial Cells

The glial cells were cultured in DMEM containing 10% FBS and 50 μg/mL gentamicin (humidified atmosphere, 5% CO_2,

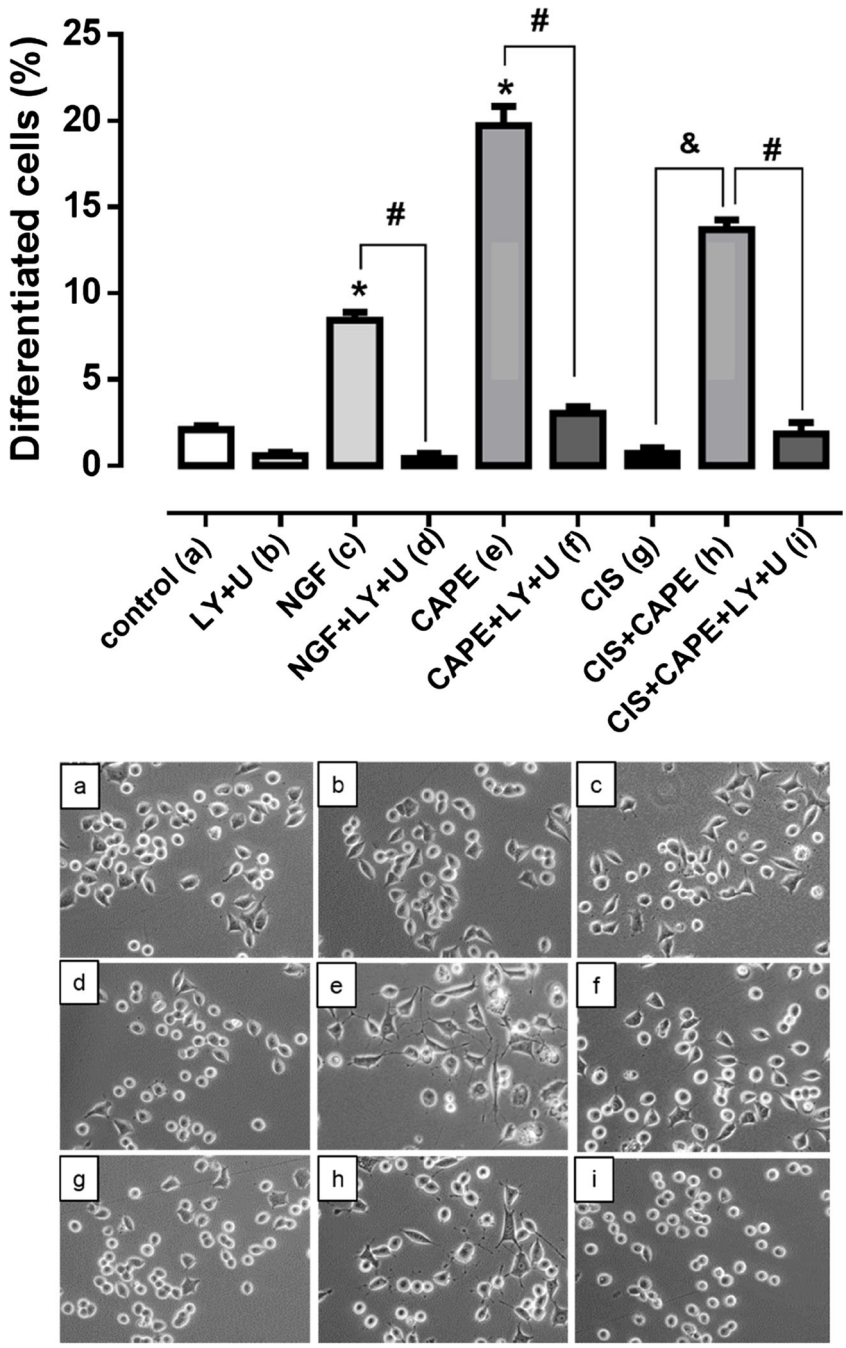

Fig. 3 Effects of the combined treatment with the inhibitors of the MAPK/Erk pathway (U0126) and PI3K/Akt pathway (LY294002) on the differentiation of PC12 cells exposed to cisplatin and/or CAPE. PC12 cells were pretreated with U0126 (10 μM) and LY294002 (30 μM) for 1 h and then treated with 100 ng/mL NGF, 5 μM cisplatin, and/or 10 μM CAPE. Inverted phase-contrast photomicrographs of (**a**) controls (untreated cells); (**b**) U0126 10 μM + LY294002; (**c**) NGF 100 ng/mL; (**d**) NGF + U0126 + LY294002; (**e**) CAPE 10 μM; (**f**) CAPE + U0126 + LY294002; (**g**) CIS; (**h**) CIS + CAPE; and (**i**) CIS + CAPE + U0126 + LY294002 after incubation for 48 h. The combined use of both inhibitors caused cell death when cells were incubated for 72 h. The number of cells with at least one neurite with the length equal to or higher than the cell body is expressed as percentage of the total cells in the field. Bars represent mean ± SEM of three different experiments performed in triplicates. *Significantly different from the untreated control group ($p < 0.05$); #significantly different from the respective control without inhibitors ($p < 0.05$); &significantly different from the cisplatin group ($p < 0.05$)

37 °C). After growth for 10 days, the cells were detached with 0.05% trypsin, centrifuged, and plated (10^4 cells/well) in poly-lysine-coated 96-well plates. Plates were cultured for 14 days, with media changed at the 7th day before the uptake assays were performed. After 14 days, glia cells were incubated with different concentrations of cisplatin (3, 30, and 300 μM) for 30 min, 12, 24, 48, and 72 h. Then, the wells were washed with PBS-CM in an ELX50 Biotek microplate washer (Winooski, VI, USA). Uptake assays were initiated by the addition of 50 nM L-[^{3}H]-glutamate, and incubation was carried on for 10 min at room temperature. Nonspecific uptake was obtained in the presence of 10 μM DL-TBOA, a potent blocker of excitatory amino acid transporters. The plates were washed twice with PBS-CM, and, then, 100 μL of scintillation cocktail was added to each well. The radioactivity was counted in a microplate scintillation and luminescence counter MicroBeta Wallac 1450 (PerkinElmer).

Statistical Analysis

Data were expressed as means ± standard error of mean (SEM). Statistical analyses were carried out by using one-

way ANOVA (analysis of variance) for multiple comparisons, followed by the Bonferroni's post-test (GraphPad Prism Software, version 5.0 for Windows, San Diego, California, USA). Values of $p < 0.05$ were considered significant. Experiments were repeated three times using cells from different cultures. The experiments of each day were performed in triplicates. Cisplatin groups were compared with untreated controls to evaluate the neurotoxic effects, whereas Cisplatin plus CAPE groups were compared with Cisplatin groups to evaluate the neuroprotection of CAPE. In order to evaluate the intrinsic effects of CAPE, CAPE alone was compared with the untreated controls.

Results

LY294002 (Blocker of PI3K/Akt Pathway) Inhibited the Cellular Differentiation Induced by CAPE in PC12 Cells and the Neuroprotective Effect of CAPE in Cells Treated with Cisplatin

The percentage of differentiated cells was higher in the groups treated with NGF 100 ng/mL or CAPE 10 μM in comparison with the untreated controls. In the groups NGF + LY294002 and CAPE + LY294002, the neuritogenic effect was inhibited in comparison to the NGF and CAPE groups, respectively. Cisplatin decreased the differentiation in NGF-stimulated cells whereas CAPE increased the differentiation of cells treated with cisplatin. Pretreatment with LY294002 abolished the neuroprotective effect of CAPE in cells treated with cisplatin. No significant differences were observed in the percentage of differentiated cells in the group treated with LY294002 in comparison with the untreated controls (Fig. 1).

U0126 (Blocker of MAPK/Erk Pathway) Inhibited the Cellular Differentiation Induced by CAPE in PC12 Cells and the Neuroprotective Effect of CAPE in Cells Treated with Cisplatin

The percentage of differentiated cells was higher in the groups treated with NGF or CAPE in comparison with the untreated controls. In the groups NGF + U0126 and CAPE + U0126, neuritogenesis was lower than in the groups NGF and CAPE, respectively. Cisplatin decreased the differentiation in NGF-stimulated cells whereas CAPE increased the differentiation of cells treated with cisplatin. Pretreatment with U0126 abolished the neuroprotective effect of CAPE against the inhibitory effect of cisplatin on neuritogenesis. No significant differences were observed in the percentage of differentiated cells in the group treated with U0126 in comparison with the untreated controls (Fig. 2).

The Combination of Both Blockers U0126 and LY294002 Inhibited the Cellular Differentiation Induced by CAPE in PC12 Cells and the Neuroprotective Effect of CAPE in Cells Treated with Cisplatin

The effects observed with the simultaneous inhibition of both pathways, PI3K/Akt and MAPK/Erk, were similar to those of each inhibitor separately; that is decreased differentiation induced by CAPE and decreased protective effect of CAPE

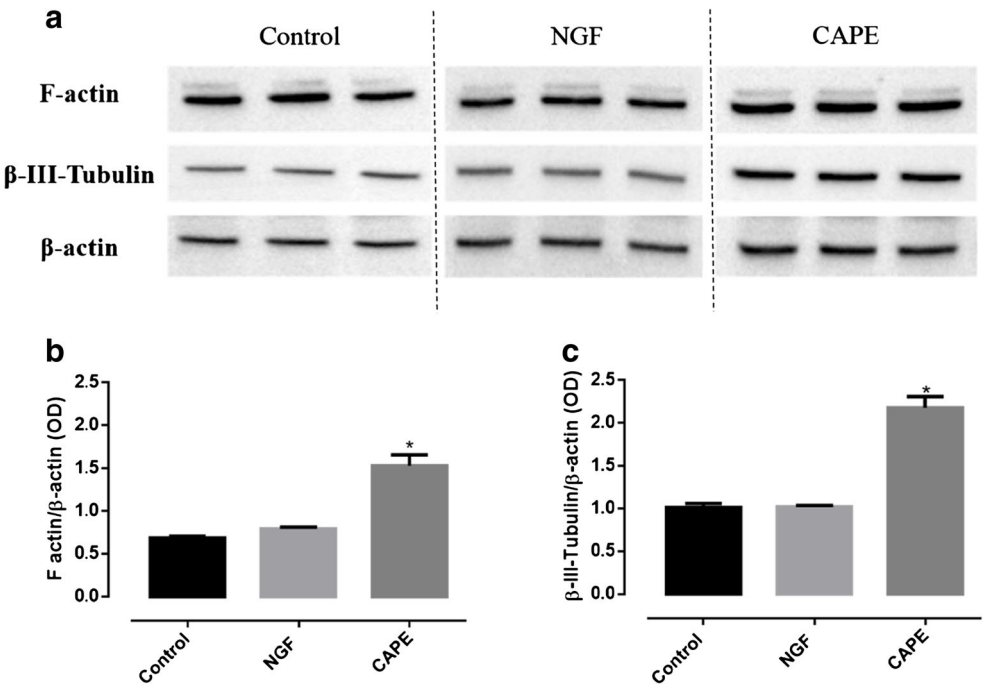

Fig. 4 Intrinsic effects of CAPE on the expression of cytoskeleton proteins (F-actin and β-III-tubulin) in PC12 cells. (**a**) Western blot bands. (**b**–**c**) Bar graphs of the normalized optical densities (OD) of (**b**) F-actin and (**c**) β-III-tubulin. Additions: NGF 100 ng/mL and CAPE 10 μM. Bars represent means ± SEM of three independent experiments performed in triplicates. *Significantly different from the control group ($p < 0.05$)

against the inhibitory effect of cisplatin (Fig. 3). However, cell death was observed when cells were incubated for periods longer than 48 h. Therefore, this assay was performed with cells incubated for 48 h, while all the other differentiation assays were performed with incubation for 72 h.

CAPE Alone Increased the Expression of the Cytoskeletal Proteins, F-Actin and β-III-Tubulin, and Protected Cells Against the Decrease Induced by Cisplatin in Both Proteins

CAPE (10 μM) increased the expression of F-actin and β-III-tubulin in non-NGF-stimulated PC12 cells in relation to untreated controls. NGF did not have any effect on the expression of both proteins in comparison with the untreated cells (Fig. 4).

CIS (5 μM) reduced the expression of F-actin and β-III-tubulin in NGF-treated cells, in comparison with the controls (treated with NGF), whereas CAPE 10 μM abolished the inhibition induced by cisplatin on the expression of both proteins, restoring the levels of controls (Fig. 5).

The Inhibition of PI3K/Akt or MAPK/Erk Pathway Did Not Alter the Expression of Cytoskeletal Proteins Induced by CAPE in PC12 Cells Treated or Not with Cisplatin

There was no significant difference in the expression of F-actin or β-III tubulin in cells treated with CAPE plus LY294002 (blocker of PI3K/Akt pathway) or CAPE plus U0126 (blocker of MAPK/Erk pathway) as compared with cells treated with CAPE alone (Fig. 6). Additionally, none of the inhibitors affected the protective effect of CAPE in the groups treated with cisplatin (Fig. 7).

Neither Cisplatin Nor CAPE Induced ROS Generation in PC12 Cells

The positive control (treated with 300 μM H_2O_2) presented a significantly higher fluorescence intensity in comparison with the control group, indicating the oxidation of the probe DCFH-DA. However, in the groups treated with CIS 5 μM and/or CAPE 10 μM, the fluorescence intensity was not different from the controls, which indicates that the concentration of ROS was unaltered in relation to the controls (Fig. 8).

Cisplatin Inhibited the Uptake of Glucose; CAPE Alone Had No Effect on the Uptake of Glucose and Neither Protected Against the Inhibition Induced by Cisplatin

In comparison with the controls, the uptake of glucose was reduced in PC12 cells treated with cytochalasin B, an inhibitor of glucose transport. CIS 5 μM also reduced the glucose uptake in comparison with the controls. CAPE (10 μM) alone had no effect on glucose uptake in comparison with the controls nor protected against the reduction induced by cisplatin (Fig. 9).

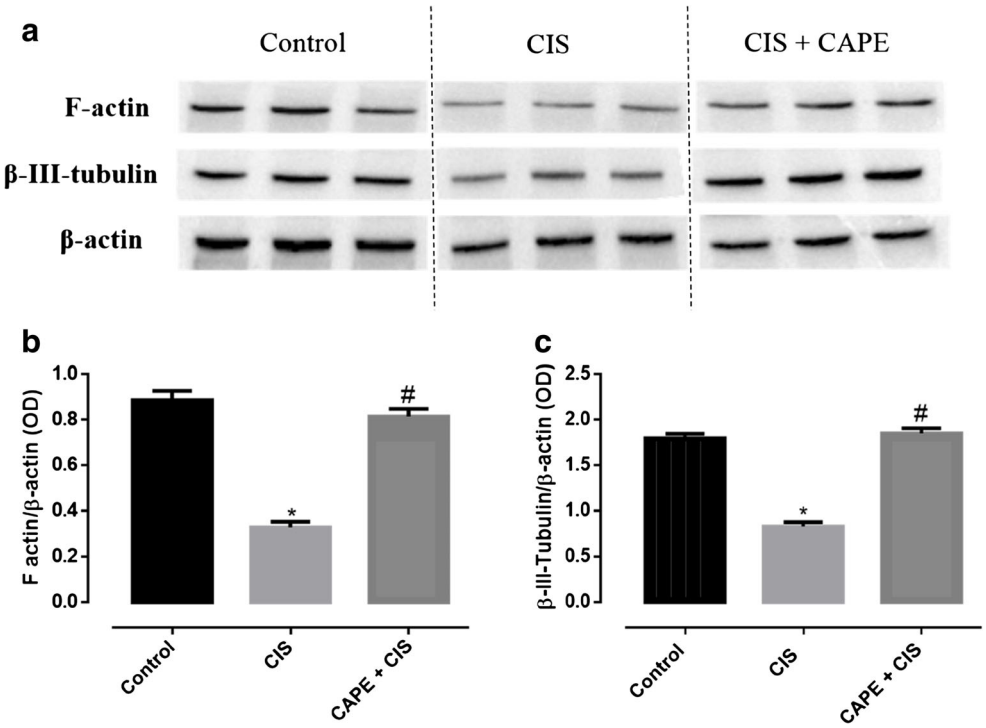

Fig. 5 Protective effect of CAPE against the reduced expression of F-actin and β-III-tubulin induced by cisplatin in PC12 cells. (**a**) Western blot bands. (**b**–**c**) Bar graphs of the normalized optical densities (OD) of (**b**) F-actin and (**c**) β-III-tubulin. Additions: NGF 100 ng/mL, CIS 5 μM, and CAPE 10 μM. Bars represent means ± SEM of three independent experiments performed in triplicates. *Significantly different from the control group ($p < 0.05$); #significantly different from the CIS group ($p < 0.05$)

CAPE Increased the Expression of the Modulators of Bioenergetics, SIRT 1 and Phospho-AMPK, and Abolished the Inhibition of SIRT 1, AMPK α, and Phospho-AMPK α Induced by Cisplatin

CAPE (10 μM) increased the expression of SIRT1 and phosphorylated AMPK α in non-NGF-stimulated PC12 cells in comparison with the controls (untreated cells). NGF increased the expression only of phosphorylated AMPK α in comparison with the untreated cells, but it had no effect on SIRT 1 or AMPK α when compared to the untreated cells (Fig. 10).

CIS (5 μM) reduced the expression of SIRT 1, AMPK α, and phospho-AMPK α in comparison with the controls (NGF-stimulated cells), while CAPE 10 μM abolished the inhibition of these proteins induced by cisplatin, restoring the control levels of AMPK α and phospho-AMPK α and surpassing the control levels of SIRT 1 (Fig. 11).

The Inhibition of the PI3K/Akt Pathway (But Not the Inhibition of the MAPK/Erk Pathway) Decreased CAPE-Induced Upregulation of SIRT1

The inhibition of the PI3K/Akt pathway induced by the pretreatment with the blocker LY294002 had no effect on the expression of AMPKα; however, it decreased the upregulation of SIRT1 induced by CAPE alone and in cells exposed to cisplatin. The inhibition of the ERK/Akt pathway (pretreatment U0126) did not affect CAPE-induced upregulation of SIRT1 or p-AMPKα in PC12 cells exposed or not to cisplatin (Fig. 12a–c and Fig. 13a–c).

Only Higher Concentrations of Cisplatin (> 60 μM) Inhibit the Uptake of L-Glutamate in EAAT2-Transfected HEK Cells and in Glial Cells (Naturally Expressing EAAT2)

First, the effect of cisplatin on the uptake of glutamate was evaluated in COS-7 cells transiently transfected with excitatory amino acid transporters (EAAT2). None of the concentrations of cisplatin evaluated (0.5–300 μM) induced a significant alteration in the uptake of glutamate in this cell model, as depicted in Fig. 14a,b. Then, the uptake of glutamate was performed in EAAT2 stably transfected HEK cells, for the evaluation of the effects of cisplatin after longer periods of incubation (up to 72 h). In this cell model, cisplatin significantly inhibited the uptake of glutamate, but only at concentrations higher than 60 μM as depicted in the bar graphs of Fig. 15a–c. The IC_{50} values for the inhibition of glutamate uptake were 66, 105, and 73 μM for 24, 48, and 72 h of incubation, respectively. It is noteworthy that the background is variable among the different concentrations of CIS applied, which suggests a non-specific inhibition of the transporters, i.e., different processes associated with glutamate uptake might be modulated by cisplatin.

The uptake of glutamate was also performed in glial cells, which naturally express EAATs. In this model, the IC_{50} was

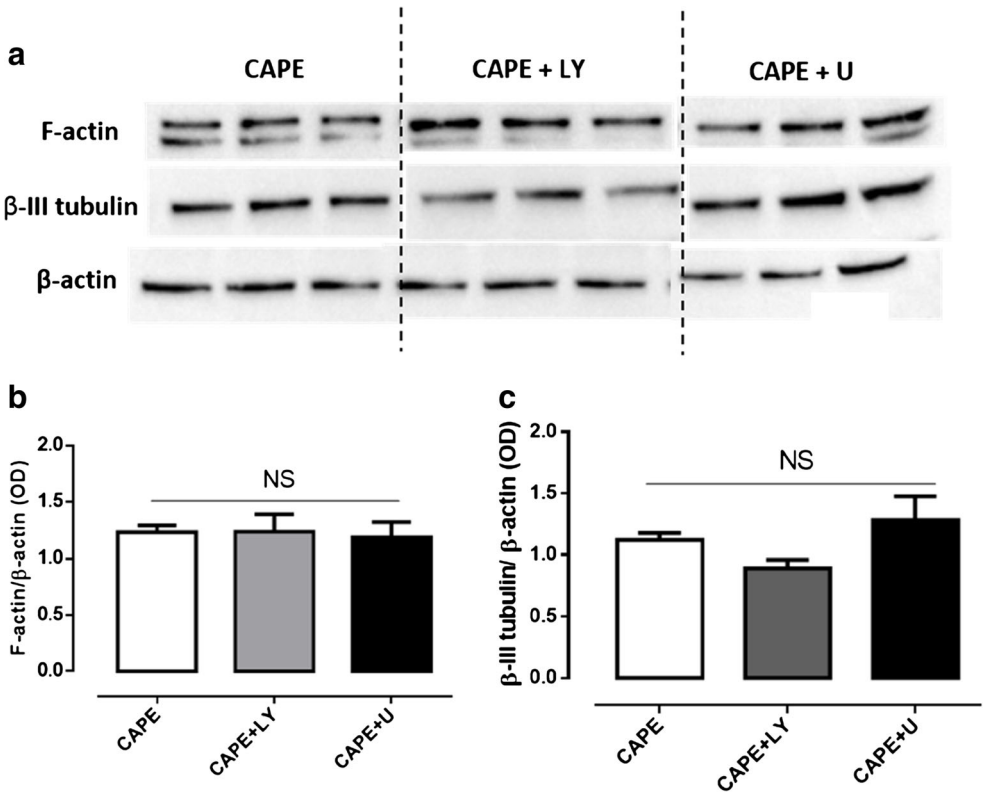

Fig. 6 Effects of CAPE on the expression of cytoskeleton proteins (F-actin and β-III-tubulin) in PC12 cells pretreated with the inhibitor of the PI3K/Akt pathway (LY294002) or the MAPK/Erk pathway (U0126). (**a**) Western blot bands. (**b**–**c**) Bar graphs of the normalized optical densities (OD) of (**b**) F-actin and (**c**) β-III-tubulin. Additions: CAPE 10 μM; LY294002; U0126. Bars represent means ± SEM of three independent experiments performed in triplicates. ^{NS}, not significantly different from the CAPE group ($p < 0.05$)

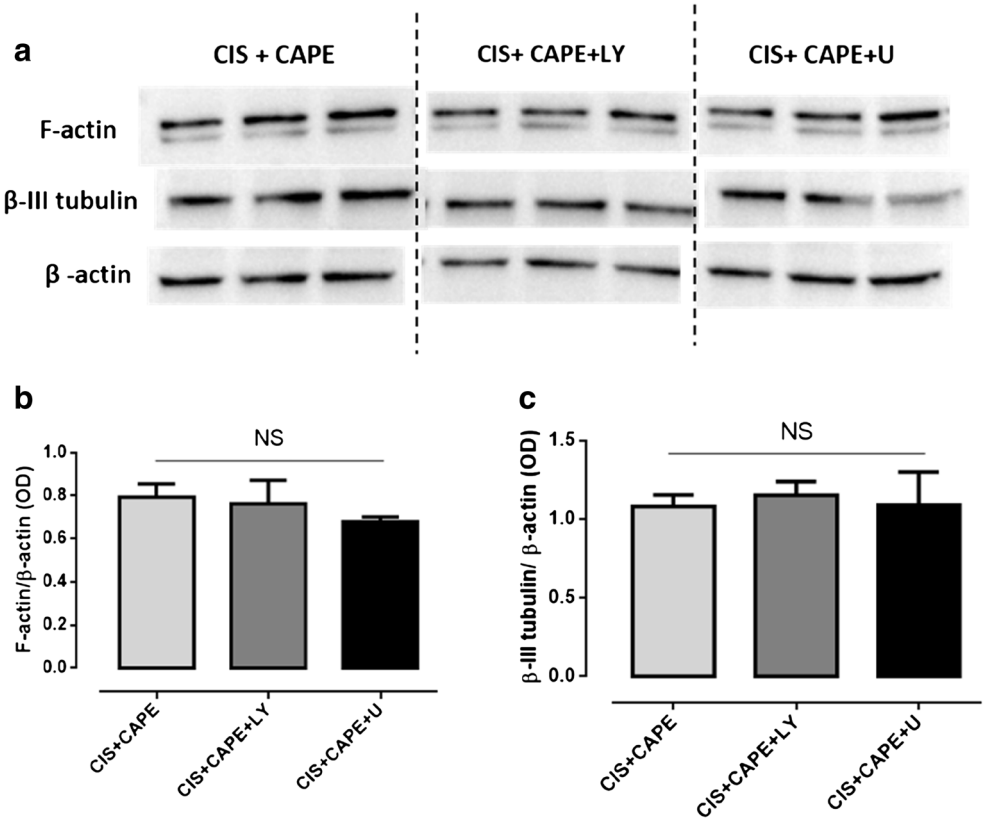

Fig. 7 Effects of CAPE on the expression of cytoskeleton proteins (F-actin and β-III-tubulin) in PC12 cells exposed to cisplatin and pretreated with the inhibitor of the PI3K/Akt pathway (LY294002) or the MAPK/Erk pathway (U0126). (**a**) Western blot bands. (**b**–**c**) Bar graphs of the normalized optical densities (OD) of (**b**) F-actin and (**c**) β-III-tubulin. Additions: cisplatin 5 μM; CAPE 10 μM; LY294002; U0126. Bars represent means ± SEM of three independent experiments performed in triplicates. ^{NS}, not significantly different from the CAPE group ($p < 0.05$)

74 μM (Fig. 16a,b). In this case, the background was obtained in the presence of TBOA, a potent blocker of the excitatory amino acid transporters (EAATs) that are naturally present in glial cells. In this cell model, no effect was observed in the background.

Altogether, these assays suggest that cisplatin, at high concentrations, has the potential to decrease the uptake of glutamate; this effect might involve the inhibition of EAATs. However, at the concentration used in the present study (5 μM), cisplatin does not interfere in the glutamate uptake, which suggests that modulation of glutamate through EAATs is not an early target of cisplatin as are the axonal proteins.

Discussion

We have reported that, in the early stage of neurotoxicity, cisplatin impairs axonal growth and synaptogenesis without inducing mitochondrial damage or apoptosis in PC12 cells (Ferreira et al. 2016). Additionally, we have demonstrated that CAPE protects against these effects by activating the NGF high-affinity receptors (trkA); this activation is induced by CAPE per se and independently of NGF (Ferreira et al. 2017). We have now used the same cell model to investigate the involvement of the signaling pathways, MAPK/Erk and PI3k/Akt, that are triggered downstream the activation of trkA receptors. Additionally, we have assessed other possible targets of peripheral neuropathies, such as axonal cytoskeletal elements (F-actin and β-III-tubulin), bioenergetics (SIRT 1, AMPK α, and p-AMPK α, glucose uptake), oxidative status (ROS generation), and glutamate transport.

The PI3K/Akt and MAPK/Erk are important signaling pathways that are activated by trkA receptors (Huang and

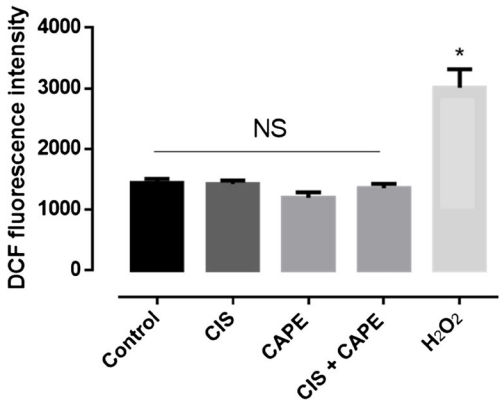

Fig. 8 Effects of cisplatin and/or CAPE on ROS generation in PC12 cells. Cells were preloaded with 100 μM DFCH-DA (30–60 min) and then treated with CIS 5 μM and/or CAPE 10 μM and incubated for 72 h. Untreated cells were used as negative controls. Cells treated with H_2O_2 300 μM were used as positive controls. The increase of dichlorofluorescein (DCF) fluorescence intensity was measured in a fluorescence microplate reader. The results are expressed as mean ± SEM of three different experiments performed in triplicates. *Significantly different from the control group ($p < 0.05$)

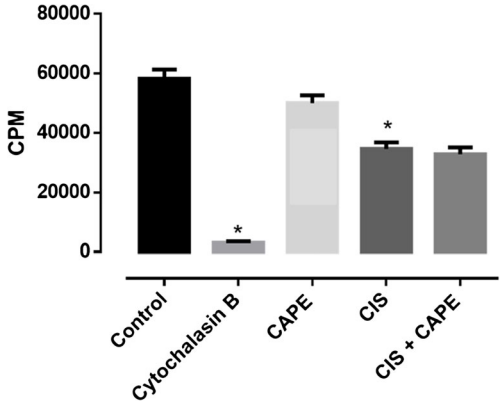

Fig. 9 Effects of cisplatin and/or CAPE on glucose uptake in PC12 cells. PC12 cells were treated with CIS 5 μM and/or CAPE 10 μM for 72 h. Then, the medium was replaced by glucose-free DMEM, and, then, the cells were treated with equimolar concentrations of radiolabeled and non-radiolabeled glucose. Untreated cells were used as negative controls. Cells treated with cytochalasin B were used as positive controls. The radioactivity was determined in a scintillation counter (Microbeta 1450 LSC Luminescence Counter), and the results were expressed as counts per minute (CPM). The results are expressed as mean ± SEM of three different experiments performed in triplicates. *Significantly different from the control group ($p < 0.05$)

Reichardt 2003). The activation of phosphatidylinositol-3-kinase (PI3K) is essential for the survival of neurons, while the activation of MAPK/Erk signaling cascade is essential for differentiation of neurons (Huang and Reichardt 2001). Here, we investigated the involvement of these pathways in the neurotrophic mechanism of CAPE by using specific inhibitors. Both PI3K inhibitor (LY294002) and MAPK inhibitor (U0126), either alone or combined, reduced the neuritogenesis induced by CAPE in PC12 cells treated or not with cisplatin. These findings clearly suggest the involvement of the neurotrophic NGF signaling pathway, i.e., activation of trkA and the downstream PI3K/Akt and MAPK/Erk pathways, in the neuroprotective mechanism of CAPE. It is noteworthy that CAPE induces these neurotrophic pathways in cells deprived of NGF besides protecting against the inhibitory effect of cisplatin on neuritogenesis.

The neuronal cytoskeleton plays an important role in axonal growth and branching during the development of the nervous system (Papandreou and Leterrier 2018). Besides that, it also plays a role in the regeneration of damaged axons (Difato et al. 2011). Actin filaments, especially F-actin, are the major determinants of axon extension and guidance (Kevenaar and Hoogenraad 2015). Actin and microtubules (formed by α and β tubulin) play a role in axon branching and the formation of filopodia, a protrusion in the neuronal cell body that precedes the formation of a neurite. In fact, the initiation of neurites requires the orchestrated accumulation, rearrangement, and polymerization of actin and microtubules at the sites of nascent neurites (Sainath and Gallo 2015).

In the present study, we demonstrated that cisplatin reduced the expression of two structural components of the cytoskeleton (F-actin and β-III-tubulin) and that CAPE protected against the decrease of these proteins induced by cisplatin, restoring the control levels. Growing evidence suggests that

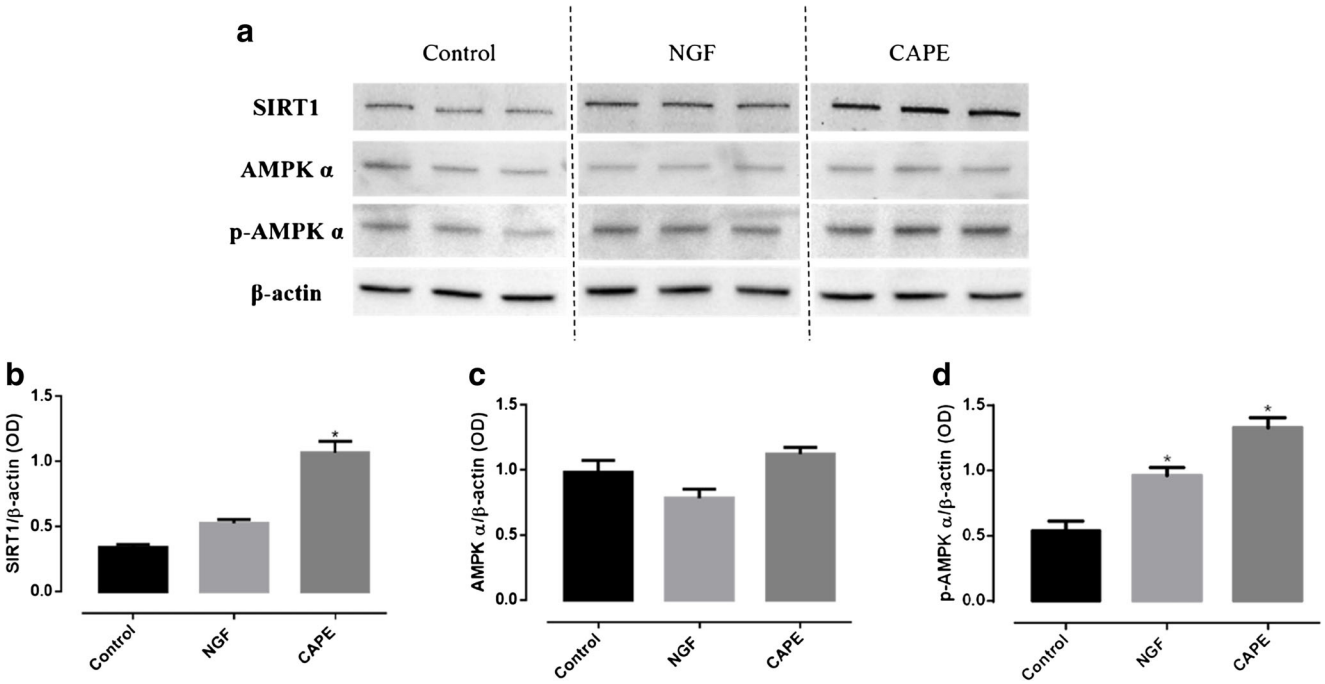

Fig. 10 Effects of CAPE on the expression of SIRT 1, AMPK α, and p-AMPK α in PC12 cells. (**a**) Western blot bands. (**b**–**d**) Bar graphs of the normalized optical densities (OD) of (**b**) SIRT 1, (**c**) AMPK α, and (**d**) p-AMPK α. Additions: NGF 100 ng/mL and CAPE 10 μM. Bars represent means ± SEM of three independent experiments performed in triplicates. *Significantly different from the control group ($p < 0.05$). p-AMPK, phosphorylated AMPK

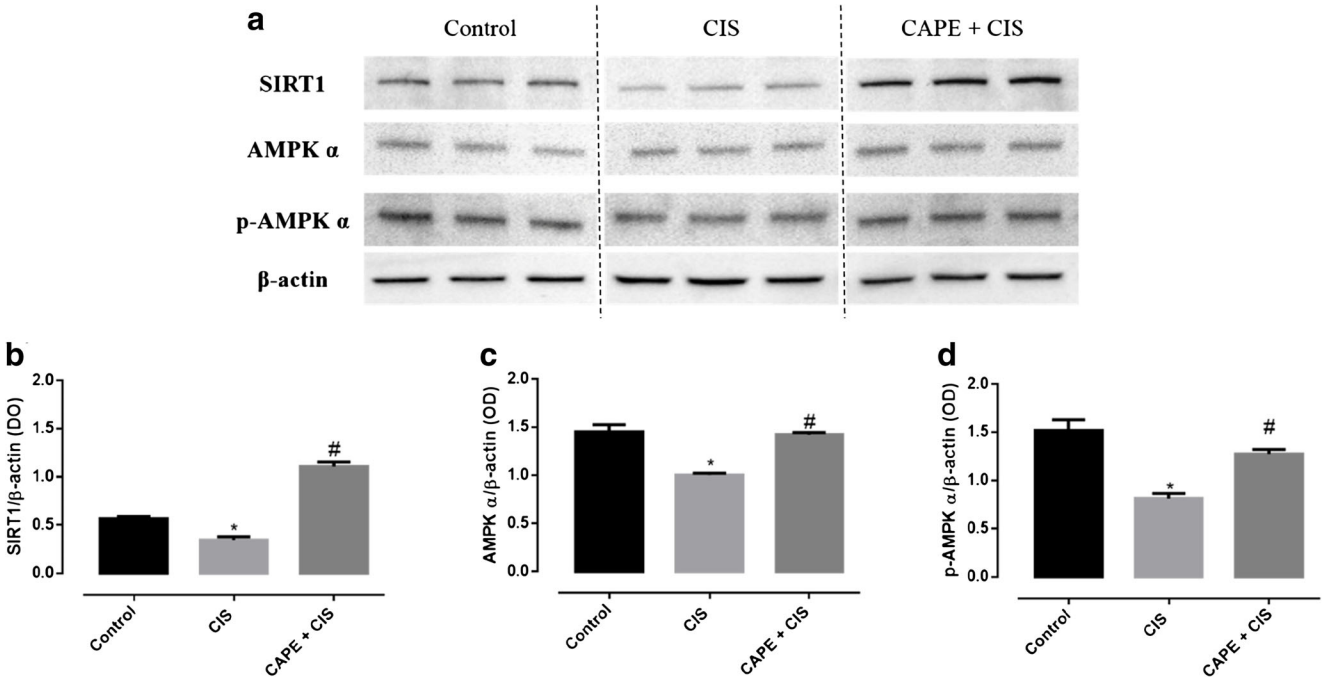

Fig. 11 Protective effect of CAPE against the reduced expression of SIRT 1, AMPK α, and p-AMPK α induced by cisplatin in PC12 cells. (**a**) Western blot bands. (**b**–**d**) Bar graphs of the normalized optical densities (OD) of (**b**) SIRT 1, (**c**) AMPK α, and (**d**) p-AMPK α. Additions: NGF 100 ng/mL, CIS 5 μM, and CAPE 10 μM. Bars represent means ± SEM of three independent experiments performed in triplicates. *Significantly different from the control group ($p < 0.05$); #significantly different from the CIS group ($p < 0.05$)

peripheral neuropathies are often associated with disturbances or alterations in the cytoskeleton (Pareyson et al. 2015; Prior et al. 2017). Altogether, our previous and present findings suggest that neuroplasticity-related proteins (Ferreira et al. 2016; Ferreira et al. 2017) and cytoskeletal proteins are targets of cisplatin that are protected by CAPE. Therefore, our findings support the potential of CAPE to regenerate damaged axons and this might indicate a beneficial effect in the

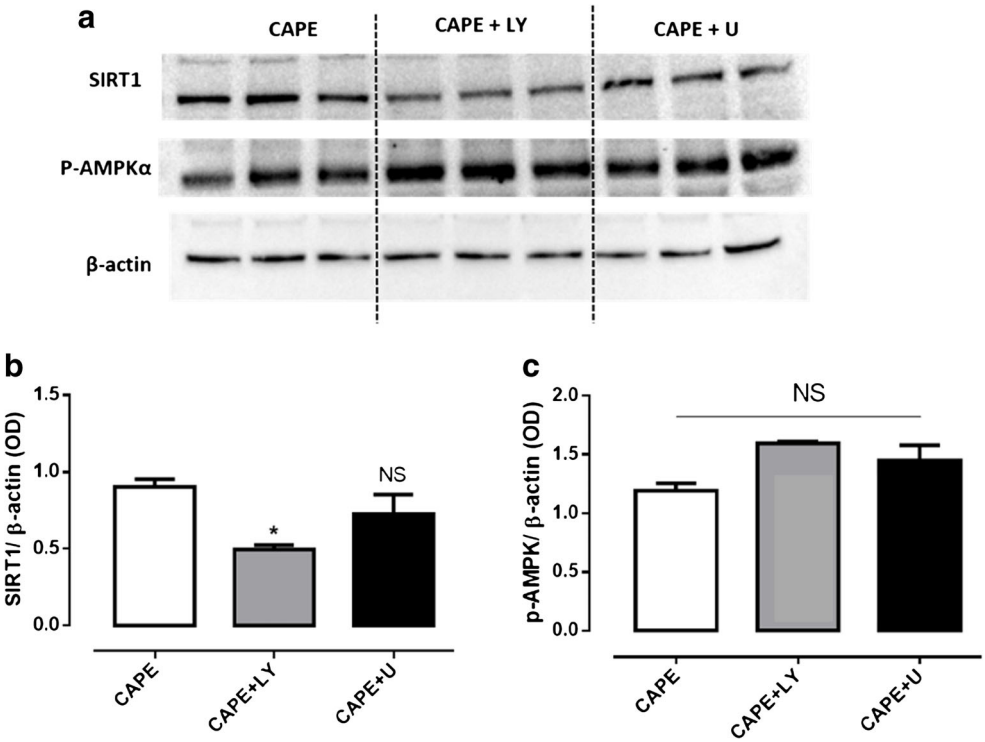

Fig. 12 Effects of CAPE on the expression of SIRT 1 and p-AMPK α in cells pretreated with the inhibitors of the PI3K/Akt pathway (LY294002) or the MAPK/Erk pathway (U0126). (**a**) Western blot bands. (**b**–**c**) Bar graphs of the normalized optical densities (OD) of (**b**) SIRT 1 and (**c**) p-AMPK α. Additions: 10 μM CAPE; 30 μM LY294002, and 10 μM U0126. Bars represent means ± SEM of three independent experiments performed in triplicates. *Significantly different from the control group ($p < 0.05$). p-AMPK, phosphorylated AMPK. NS, not significantly different from the CAPE group ($p < 0.05$)

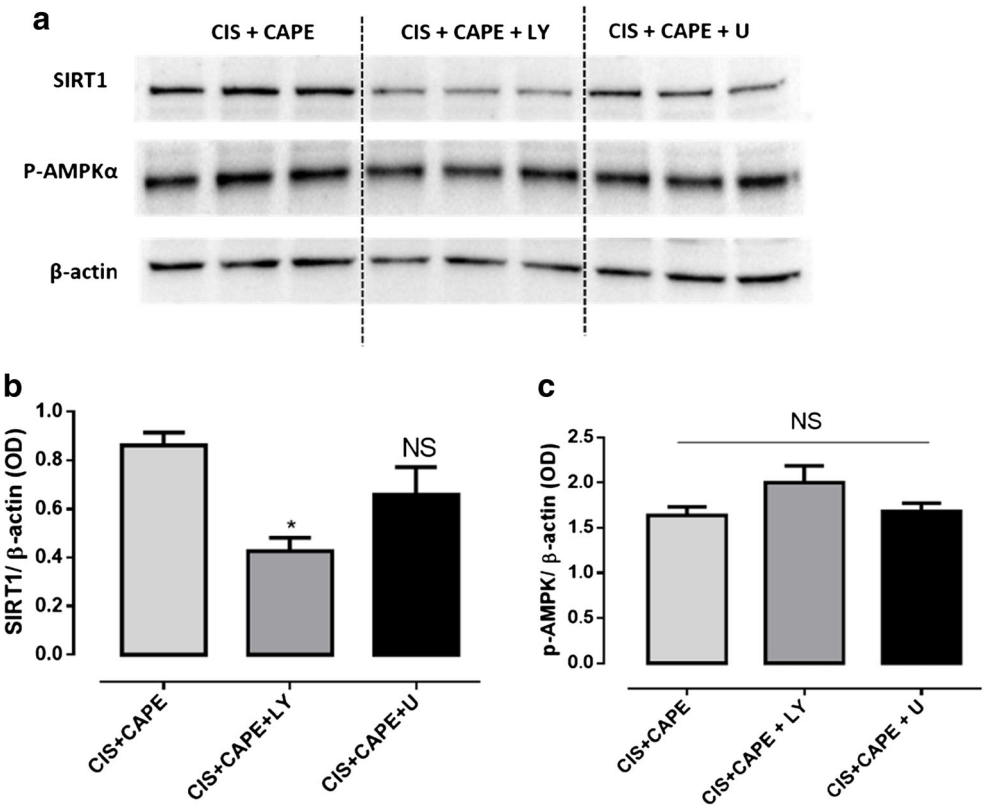

Fig. 13 Effects of CAPE on the expression of SIRT 1 and p-AMPK α in cells exposed to cisplatin and pretreated with the inhibitor of the PI3K/Akt pathway (LY294002) or the MAPK/Erk pathway (U0126). (**a**) Western blot bands. (**b**–**c**) Bar graphs of the normalized optical densities (OD) of (**b**) SIRT 1 and (**c**) p-AMPK α. Additions: cisplatin 5 μM; CAPE 10 μM; LY294002 and U0126. Bars represent means ± SEM of three independent experiments performed in triplicates. *Significantly different from the control group ($p < 0.05$). p-AMPK, phosphorylated AMPK. NS, not significantly different from the CIS + CAPE group ($p < 0.05$)

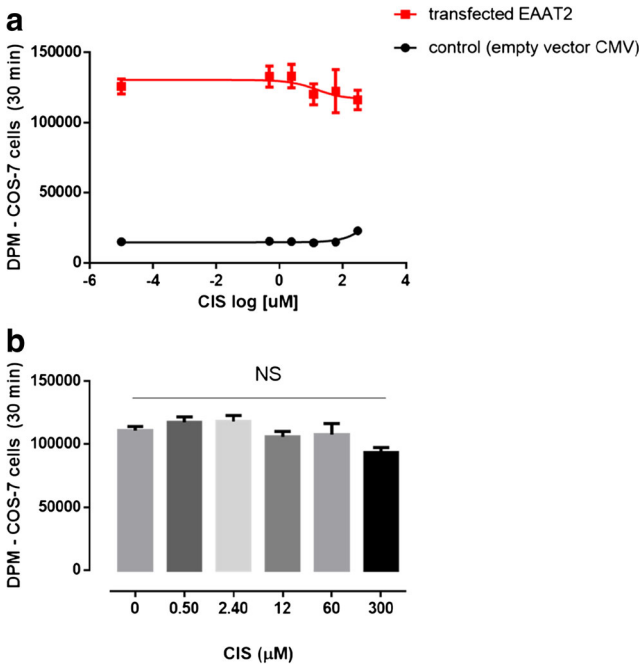

Fig. 14 Effect of cisplatin on the uptake of glutamate in COS-7 cells transfected with the glutamate transporter EAAT2 (excitatory amino acid transporter 2). Cells were incubated with different concentrations of cisplatin (0.50, 2.4, 12, 60, and 300 μM) for 30 min. Controls were incubated with empty vector CMV. No significant effect was observed in this model of transient transfection. (**a**) Concentration–response curve. (**b**) Bar graphs represent the means ± SEM of three independent experiments. NS, non-significant. CMV, cytomegalovirus

peripheral neuropathy induced by cisplatin. Interestingly, CAPE alone also increased the expression of F-actin and β-III-tubulin, while NGF did not, which suggests that CAPE might activate mechanisms other than the neurotrophic pathways (PI3k/Akt and MAPK/Erk) triggered by NGF through trkA activation. Accordingly, the inhibition of these pathways did not affect CAPE-induced upregulation of F-actin or β-III-tubulin in PC12 cells exposed or not to cisplatin.

Besides the structural damage of axonal cytoskeleton, other events associated with peripheral neurotoxicity are bioenergetics failure and oxidative stress (Melli et al. 2008). Although oxidative stress has been implicated in cisplatin-induced nephrotoxicity and hepatotoxicity (Martins et al. 2008; Santos et al. 2007), no increase in ROS production was observed after incubation of PC12 cells with cisplatin 5 μM for 72 h. On the other hand, cisplatin reduced glucose uptake, another event related to energy failure. Glucose is a major source of energy for cells, and the nervous system, in particular, requires a continuous supply of glucose to maintain its metabolic homeostasis (Verberne et al. 2014). The uptake of glucose by GLUTs (glucose transporters) is dependent on actin from the cytoskeleton (Bunn et al. 1999); therefore, the reduced levels of cytoskeleton proteins (F-actin and β-III-tubulin) might explain the reduced glucose uptake induced by cisplatin in our study. In fact, a study suggested that cisplatin binds to tubulin and affects the localization of GLUT1 in the plasma membrane, reducing glucose uptake without

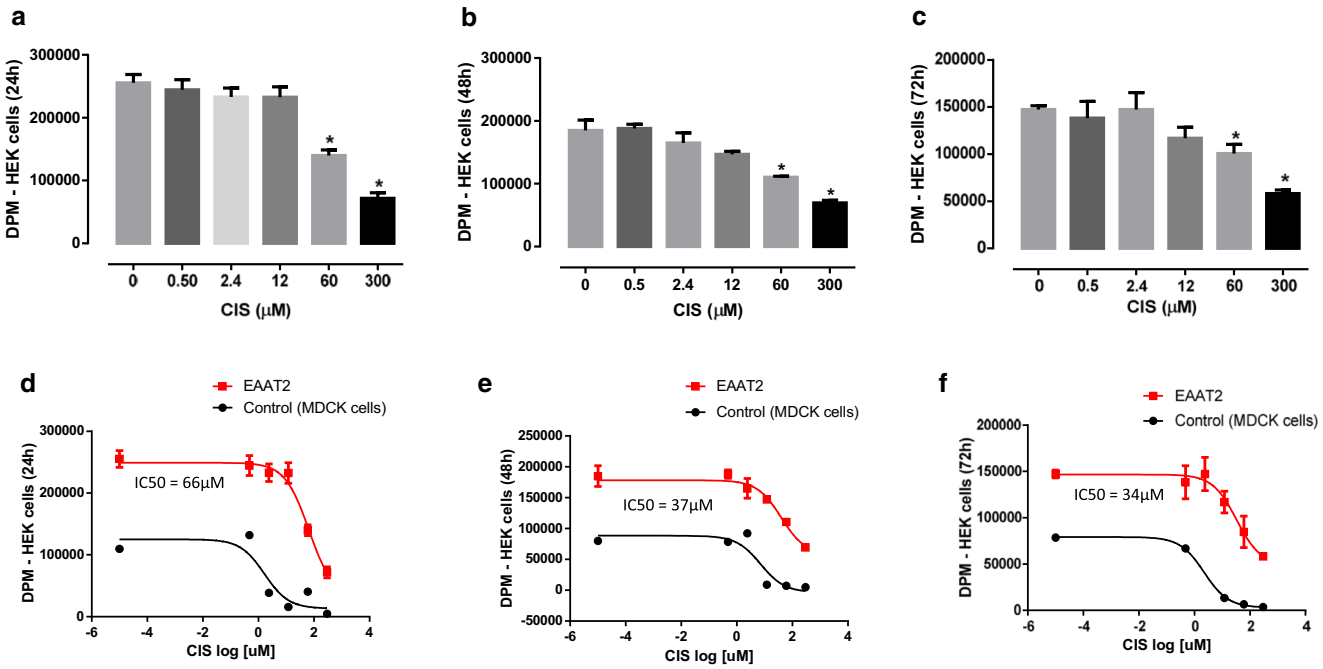

Fig. 15 Effect of cisplatin on glutamate uptake in HEK cells. Assays were performed in HEK cells stably transfected with EAAT2. MDCK-naïve cells were used as controls. Cells were incubated with different concentrations of cisplatin (0.50, 2.4, 12, 60, and 300 μM) for (**a**) 24 h, (**b**) 48 h, and (**c**) 72 h. Uptake was triggered by the addition of 50 nM L-[^{3}H]-glutamate. (**a**–**c**) Bar graphs represent the means ± SEM of three independent experiments. (**d**–**f**) Concentration–response curve after incubation with cisplatin for (**a**) 24 h (IC_{50} = 66 μM), (**b**) 48 h (IC_{50} = 37 μM), and (**c**) 72 h (IC_{50} = 34 μM)

interfering with membrane integrity or mitochondrial function (Egawa-Takata et al. 2010). This is in accordance with our findings; we have previously demonstrated that cisplatin (5 μM) did not alter the mitochondrial function neither induced apoptosis in PC12 cells (Ferreira et al. 2016). Now, we have demonstrated that, at the same concentration (5 μM), cisplatin reduces the uptake of glucose without increasing ROS, an event closely related to mitochondrial damage. These findings indicate that, although being damaged by cisplatin, mitochondria are not its primary targets, as are the axonal proteins and glucose uptake. Although CAPE protected the cytoskeleton proteins against the effects of cisplatin, it did not protect against the reduction of glucose uptake induced by cisplatin, nor improved the uptake of glucose when added alone to PC12 cells. Different from our results, a study showed that CAPE was able to stimulate glucose uptake, but in skeletal muscle cells (Lee et al. 2007), which might be attributed to differences in GLUT subtypes in different cells. In PC12 cells and neurons, glucose uptake relies on GLUT3 (Heather West Greenlee et al. 2003); however, in muscle cells, the glucose uptake increases after the translocation of the GLUT4 to the plasma membrane (Czech and Corvera 1999; Pessin and Bell 1992).

Since cisplatin reduced the glucose uptake in PC12 cells, we investigated the expression of two key proteins related to bioenergetics, AMPK and SIRT1. The AMP-activated protein

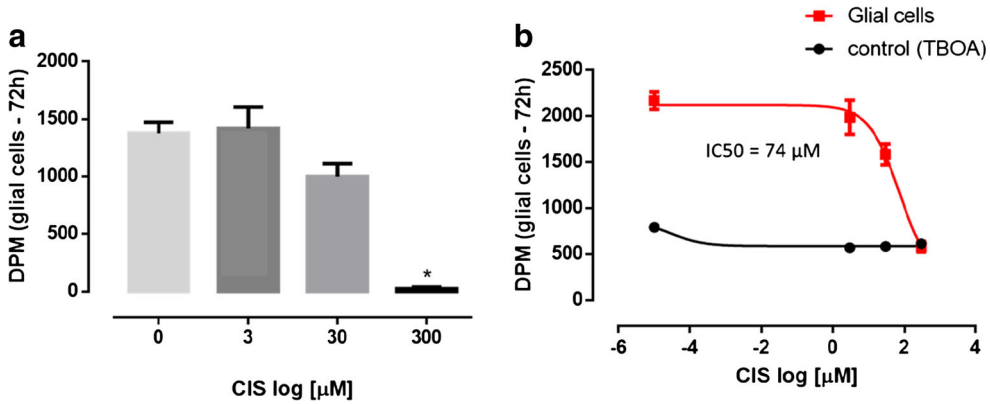

Fig. 16 Effect of cisplatin on the uptake of glutamate by glial cells. Cells were incubated with different concentrations of cisplatin (3, 30, and 300 μM) for 72 h. Controls were treated with TBOA, a blocker of EAATs. The uptake assay was initiated with the addition of 50 nM L-[^{3}H]-glutamate. (**a**) Bar graph represents the means ± SEM of three independent experiments. (**b**) Concentration–response curve (IC_{50} = 74 μM)

kinase (AMPK) regulates the cell metabolism according to nutrient availability. The activated form of AMPK (p-AMPK) is the molecule phosphorylated at the threonine 172 in the α subunit. It stimulates glucose uptake by phosphorylating molecules that promote GLUT translocation to plasma membranes (Herzig and Shaw 2018; Ronnett et al. 2009). Energy balance and glucose metabolism are also regulated by SIRT1 1 (Sirtuin), the most conserved mammalian NAD^+-dependent deacetylase (Li 2013). Besides that, SIRT1 is critical for the survival, proliferation (Li and Wang 2017), and synaptic plasticity of neuronal cells (Min et al. 2013; Lu et al. 2013). Cisplatin reduced the expression of AMPK α, p-AMPK α, and SIRT1 in PC12 cells, suggesting that these energy-related proteins are early targets of cisplatin. Interferences in AMPK and SIRT1 protein expressions after cisplatin treatment were previously associated with the mechanism of nephrotoxicity of cisplatin (Wilmes et al. 2015; Kim et al. 2011); here, we show their implication in the neurotoxicity of cisplatin, as well. CAPE increased the expression of phosphorylated-AMPK (p-AMPK α), without altering the expression of AMPK α, which suggests that CAPE activates AMPK α by inducing its phosphorylation. Accordingly, a study in BV-2 murine microglial cells showed the participation of AMPK α in the protective effect of CAPE (Tsai et al. 2015). Furthermore, CAPE per se increased the expression of SIRT1, and, in cells treated with cisplatin, CAPE minimized the downregulation induced by cisplatin on the expression of AMPK α, p-AMPK α, and SIRT1. The inhibition of the neurotrophic pathway, PI3K/Akt, reduced CAPE-induced upregulation of SIRT1 in cells treated or not with cisplatin. Similarly, a study in PC12 cells showed that the panaxatriol saponin (PTS)-upregulated expression of SIRT1 was attenuated by the inhibition of the PI3K/Akt pathway, suggesting a crosstalk between AKT and SIRT1 (Zhang et al. 2017). On the other hand, results do not suggest any crosstalk between the neurotrophic MAPK/Erk pathway and the energy-related AMPK/SIRT1 pathway.

Bioenergetics failure also affects the uptake of glutamate by the excitatory amino acid transporters (EAATs), leading to overactivation of the post-synaptic receptors (Attwell et al. 1993; Carozzi et al. 2008a). Glutamate is the predominant excitatory neurotransmitter in the central nervous system (CNS), but studies have demonstrated that glutamate signaling also plays a role in the peripheral nervous system (Walker et al. 2001; Carozzi et al. 2008b). The inhibition of glutamate carboxypeptidase II—the enzyme responsible for glutamate production—reduced the severity of cisplatin-induced peripheral neuropathy in rats (Carozzi et al. 2010). However, little is known about the role of glutamate transporters in peripheral neuropathies (Carozzi et al. 2008a). Therefore, we investigated the involvement of glutamate transporters in the neurotoxicity of cisplatin, by assessing the effect of cisplatin on glutamate uptake. Only high concentrations of cisplatin (above 60 μM) decreased the uptake of glutamate; at the concentration of the present study (5 μM), cisplatin does not alter the glutamate uptake, which suggests that glutamate uptake is not an early target of cisplatin.

Conclusion

The axonal cytoskeletal proteins (F-actin and β-III-tubulin), energy-related proteins (AMPK α, p-AMPK α, and SIRT1), and glucose uptake are early targets of cisplatin. CAPE minimizes the inhibitory effects of cisplatin on the axonal proteins, SIRT1, AMPK, and p-AMPK, but has no beneficial effect on glucose uptake. The mechanism of neuroprotection of CAPE involves the activation of the same neurotrophic signaling pathways triggered by NGF (PI3k/Akt and MAPK/Erk pathways). The activation of PI3K/Akt pathway seems to be important for the upregulation of SIRT1 (but not of other proteins) induced by CAPE. Excitotoxicity of glutamate and oxidative stress are not involved in the early axonal damage caused by cisplatin.

Acknowledgements The authors are thankful to CNPq (Conselho Nacional de Desenvolvimento Científico e Tecnológico, grant number 140106/2015-4) and FAPESP (Fundação de Amparo à Pesquisa do Estado de São Paulo, grant number 2017/09332-7) for the financial support.

Compliance with Ethical Standards

Conflict of Interest The authors declare that there are no conflicts of interest.

References

Abdul Muneer PM, Alikunju S, Szlachetka AM, Mercer AJ, Haorah J (2011) Ethanol impairs glucose uptake by human astrocytes and neurons: protective effects of acetyl-L-carnitine. Int J Physiol Pathophysiol Pharmacol 3:48–56

Areti A, Yerra VG, Naidu V, Kumar A (2014) Oxidative stress and nerve damage: role in chemotherapy induced peripheral neuropathy. Redox Biol 2:289–295

Argyriou AA, Bruna J, Marmiroli P, Cavaletti G (2012) Chemotherapy-induced peripheral neurotoxicity (CIPN): an update. Crit Rev Oncol Hematol 82:51–77

Asbury AK (1987) Sensory neuronopathy. Semin Neurol 7:58–66

Attwell D, Barbour B, Szatkowski M (1993) Nonvesicular release of neurotransmitter. Neuron 11:401–407

Bunn RC, Jensen MA, Reed BC (1999) Protein interactions with the glucose transporter binding protein GLUT1CBP that provide a link between GLUT1 and the cytoskeleton. Mol Biol Cell 10:819–832

Carozzi V, Marmiroli P, Cavaletti G (2008a) Focus on the role of glutamate in the pathology of the peripheral nervous system. CNS Neurol Disord Drug Targets 7:348–360

Carozzi VA, Canta A, Oggioni N, Ceresa C, Marmiroli P, Konvalinka J, Zoia C, Bossi M, Ferrarese C, Tredici G, Cavaletti G (2008b) Expression and distribution of 'high affinity' glutamate transporters

GLT1, GLAST, EAAC1 and of GCPII in the rat peripheral nervous system. J Anat 213:539–546

Carozzi VA, Ceresa C (2012) The role of glutamate in diabetic and in chemotherapy induced peripheral neuropathies and its regulation by glutamate carboxypeptidase II. Curr Med Chem 19:1261–1268

Carozzi VA, Chiorazzi A, Canta A, Lapidus RG, Slusher BS, Wozniak KM, Cavaletti G (2010) Glutamate carboxypeptidase inhibition reduces the severity of chemotherapy-induced peripheral neurotoxicity in rat. Neurotox Res 17:380–391

Czech MP, Corvera S (1999) Signaling mechanisms that regulate glucose transport. J Biol Chem 274:1865–1868

Das KP, Freudenrich TM, Mundy WR (2004) Assessment of PC12 cell differentiation and neurite growth: a comparison of morphological and neurochemical measures. Neurotoxicol Teratol 26:397–406

Difato F, Tsushima H, Pesce M, Benfenati F, Blau A, Chieregatti E (2011) The formation of actin waves during regeneration after axonal lesion is enhanced by BDNF. Sci Rep 1:183

Ebstensen RD, Plagemann PG (1972) Cytochalasin B: inhibition of glucose and glucosamine transport. Proc Natl Acad Sci U S A 69:1430–1434

Egawa-Takata T, Endo H, Fujita M, Ueda Y, Miyatake T, Okuyama H, Yoshino K, Kamiura S, Enomoto T, Kimura T, Inoue M (2010) Early reduction of glucose uptake after cisplatin treatment is a marker of cisplatin sensitivity in ovarian cancer. Cancer Sci 101:2171–2178

Ferreira RS, Dos Santos NA, Martins NM, Fernandes LS, Dos Santos AC (2016) Non-cytotoxic concentration of cisplatin decreases neuroplasticity-related proteins and neurite outgrowth without affecting the expression of NGF in PC12 cells. Neurochem Res 41: 2993–3003

Ferreira RS, Dos Santos NAG, Martins NM, Fernandes LS, Dos Santos AC (2017) Caffeic acid phenethyl ester (CAPE) protects PC12 cells from cisplatin-induced neurotoxicity by activating the NGF-signaling pathway. Neurotox Res

Gregg RW, Molepo JM, Monpetit VJ, Mikael NZ, Redmond D, Gadia M, Stewart DJ (1992) Cisplatin neurotoxicity: the relationship between dosage, time, and platinum concentration in neurologic tissues, and morphologic evidence of toxicity. J Clin Oncol 10:795–803

Heather West Greenlee M, Uemura E, Carpenter SL, Doyle RT, Buss JE (2003) Glucose uptake in PC12 cells: GLUT3 vesicle trafficking and fusion as revealed with a novel GLUT3-GFP fusion protein. J Neurosci Res 73:518–525

Herzig S, Shaw RJ (2018) AMPK: guardian of metabolism and mitochondrial homeostasis. Nat Rev Mol Cell Biol 19:121–135

Huang EJ, Reichardt LF (2001) Neurotrophins: roles in neuronal development and function. Annu Rev Neurosci 24:677–736

Huang EJ, Reichardt LF (2003) Trk receptors: roles in neuronal signal transduction. Annu Rev Biochem 72:609–642

Inno A, Di Noia V, D'Argento E, Modena A, Gori S (2016) State of the art of chemotherapy for the treatment of central nervous system metastases from non-small cell lung cancer. Transl Lung Cancer Res 5:599–609

Johnson C, Pankratz VS, Velazquez AI, Aakre JA, Loprinzi CL, Staff NP, Windebank AJ, Yang P (2015) Candidate pathway-based genetic association study of platinum and platinum-taxane related toxicity in a cohort of primary lung cancer patients. J Neurol Sci 349:124–128

Kanat O, Evrensel T, Baran I, Coskun H, Zarifoglu M, Turan OF, Kurt E, Demiray M, Gonullu G, Manavoglu O (2003) Protective effect of amifostine against toxicity of paclitaxel and carboplatin in non-small cell lung cancer: a single center randomized study. Med Oncol 20: 237–245

Kevenaar JT, Hoogenraad CC (2015) The axonal cytoskeleton: from organization to function. Front Mol Neurosci 8:44

Kim DH, Jung YJ, Lee JE, Lee AS, Kang KP, Lee S, Park SK, Han MK, Lee SY, Ramkumar KM, Sung MJ, Kim W (2011) SIRT1 activation by resveratrol ameliorates cisplatin-induced renal injury through deacetylation of p53. Am J Physiol Ren Physiol 301:F427–F435

Krarup-Hansen A, Helweg-Larsen S, Schmalbruch H, Rorth M, Krarup C (2007) Neuronal involvement in cisplatin neuropathy: prospective clinical and neurophysiological studies. Brain 130:1076–1088

L'Episcopo F, Serapide MF, Tirolo C, Testa N, Caniglia S, Morale MC, Pluchino S, Marchetti B (2011) A Wnt1 regulated Frizzled-1/beta-catenin signaling pathway as a candidate regulatory circuit controlling mesencephalic dopaminergic neuron-astrocyte crosstalk: therapeutical relevance for neuron survival and neuroprotection. Mol Neurodegener 6:49

Lee ES, Uhm KO, Lee YM, Han M, Lee M, Park JM, Suh PG, Park SH, Kim HS (2007) CAPE (caffeic acid phenethyl ester) stimulates glucose uptake through AMPK (AMP-activated protein kinase) activation in skeletal muscle cells. Biochem Biophys Res Commun 361: 854–858

Li H, Wang R (2017) Blocking SIRT1 inhibits cell proliferation and promotes aging through the PI3K/AKT pathway. Life Sci 190:84–90

Li X (2013) SIRT1 and energy metabolism. Acta Biochim Biophys Sin Shanghai 45:51–60

Liu E, Du X, Ge R, Liang T, Niu Q, Li Q (2013) Comparative toxicity and apoptosis induced by diorganotins in rat pheochromocytoma (PC12) cells. Food Chem Toxicol 60:302–308

Lu M, Sarruf DA, Li P, Osborn O, Sanchez-Alavez M, Talukdar S, Chen A, Bandyopadhyay G, Xu J, Morinaga H, Dines K, Watkins S, Kaiyala K, Schwartz MW, Olefsky JM (2013) Neuronal Sirt1 deficiency increases insulin sensitivity in both brain and peripheral tissues. J Biol Chem 288:10722–10735

Lykissas MG, Batistatou AK, Charalabopoulos KA, Beris AE (2007) The role of neurotrophins in axonal growth, guidance, and regeneration. Curr Neurovasc Res 4:143–151

Martins NM, Santos NA, Curti C, Bianchi ML, Santos AC (2008) Cisplatin induces mitochondrial oxidative stress with resultant energetic metabolism impairment, membrane rigidification and apoptosis in rat liver. J Appl Toxicol 28:337–344

McDonald ES, Randon KR, Knight A, Windebank AJ (2005) Cisplatin preferentially binds to DNA in dorsal root ganglion neurons in vitro and in vivo: a potential mechanism for neurotoxicity. Neurobiol Dis 18:305–313

Melli G, Taiana M, Camozzi F, Triolo D, Podini P, Quattrini A, Taroni F, Lauria G (2008) Alpha-lipoic acid prevents mitochondrial damage and neurotoxicity in experimental chemotherapy neuropathy. Exp Neurol 214:276–284

Min SW, Sohn PD, Cho SH, Swanson RA, Gan L (2013) Sirtuins in neurodegenerative diseases: an update on potential mechanisms. Front Aging Neurosci 5:53

Papandreou MJ, Leterrier C (2018) The functional architecture of axonal actin. Mol Cell Neurosci 91:151–159

Pareyson D, Saveri P, Sagnelli A, Piscosquito G (2015) Mitochondrial dynamics and inherited peripheral nerve diseases. Neurosci Lett 596:66–77

Park SB, Krishnan AV, Lin CS, Goldstein D, Friedlander M, Kiernan MC (2008) Mechanisms underlying chemotherapy-induced neurotoxicity and the potential for neuroprotective strategies. Curr Med Chem 15:3081–3094

Pessin JE, Bell GI (1992) Mammalian facilitative glucose transporter family: structure and molecular regulation. Annu Rev Physiol 54: 911–930

Podratz JL, Knight AM, Ta LE, Staff NP, Gass JM, Genelin K, Schlattau A, Lathroum L, Windebank AJ (2011) Cisplatin induced mitochondrial DNA damage in dorsal root ganglion neurons. Neurobiol Dis 41:661–668

Prior R, Van Helleputte L, Benoy V, Van Den Bosch L (2017) Defective axonal transport: a common pathological mechanism in inherited and acquired peripheral neuropathies. Neurobiol Dis 105:300–320

Rasband WS (1997–2018) ImageJ. U. S. National Institutes of Health, Bethesda, Maryland, USA https://imagej.nih.gov/ij/

Ronnett GV, Ramamurthy S, Kleman AM, Landree LE, Aja S (2009) AMPK in the brain: its roles in energy balance and neuroprotection. J Neurochem 109(Suppl 1):17–23

Sadri S, Bahrami F, Khazaei M, Hashemi M, Asgari A (2010) Cannabinoid receptor agonist WIN-55,212-2 protects differentiated PC12 cells from organophosphorus- induced apoptosis. Int J Toxicol 29:201–208

Sainath R, Gallo G (2015) Cytoskeletal and signaling mechanisms of neurite formation. Cell Tissue Res 359:267–278

Santos NA, Catao CS, Martins NM, Curti C, Bianchi ML, Santos AC (2007) Cisplatin-induced nephrotoxicity is associated with oxidative stress, redox state unbalance, impairment of energetic metabolism and apoptosis in rat kidney mitochondria. Arch Toxicol 81:495–504

Shimizu S, Abt A & Meucci O. 2011. Bilaminar co-culture of primary rat cortical neurons and glia. J Vis Exp.

Shirmanova MV, Druzhkova IN, Lukina MM, Dudenkova VV, Ignatova NI, Snopova LB, Shcheslavskiy VI, Belousov VV, Zagaynova EV (2017) Chemotherapy with cisplatin: insights into intracellular pH and metabolic landscape of cancer cells in vitro and in vivo. Sci Rep 7:8911

Siegal T, Haim N (1990) Cisplatin-induced peripheral neuropathy. Frequent off-therapy deterioration, demyelinating syndromes, and muscle cramps. Cancer 66:1117–1123

Starobova H, Vetter I (2017) Pathophysiology of chemotherapy-induced peripheral neuropathy. Front Mol Neurosci 10:174

Stevens MJ, Obrosova I, Cao X, Van Huysen C, Greene DA (2000) Effects of DL-alpha-lipoic acid on peripheral nerve conduction, blood flow, energy metabolism, and oxidative stress in experimental diabetic neuropathy. Diabetes 49:1006–1015

Tsai CF, Kuo YH, Yeh WL, Wu CY, Lin HY, Lai SW, Liu YS, Wu LH, Lu JK, Lu DY (2015) Regulatory effects of caffeic acid phenethyl ester on neuroinflammation in microglial cells. Int J Mol Sci 16:5572–5589

Verberne AJ, Sabetghadam A, Korim WS (2014) Neural pathways that control the glucose counterregulatory response. Front Neurosci 8:38

Walker K, Reeve A, Bowes M, Winter J, Wotherspoon G, Davis A, Schmid P, Gasparini F, Kuhn R, Urban L (2001) mGlu5 receptors and nociceptive function II. mGlu5 receptors functionally expressed on peripheral sensory neurones mediate inflammatory hyperalgesia. Neuropharmacology 40:10–19

Wilmes A, Bielow C, Ranninger C, Bellwon P, Aschauer L, Limonciel A, Chassaigne H, Kristl T, Aiche S, Huber CG, Guillou C, Hewitt P, Leonard MO, Dekant W, Bois F, Jennings P (2015) Mechanism of cisplatin proximal tubule toxicity revealed by integrating transcriptomics, proteomics, metabolomics and biokinetics. Toxicol in Vitro 30:117–127

Zhang C, Li C, Chen S, Li Z, Ma L, Jia X, Wang K, Bao J, Liang Y, Chen M, Li P, Su H, Lee SMY, Liu K, Wan JB, & He C (2017) Hormetic effect of panaxatriol saponins confers neuroprotection in PC12 cells and zebrafish through PI3K/AKT/mTOR and AMPK/SIRT1/FOXO3 pathways. Sci Rep 7:41082–41082